Polymer Vol. 37 No. 13, pp. 2609–2613, 1996

0032-3861/96/$15.00 + 0.00

The influence of polymerization rate on conductivity and crystallinity of electropolymerized polypyrrole

P. Dyreklev, M. Granström* and O. Inganäs
Laboratory of Applied Physics, Department of Physics (IFM), Linköping University, S-581 83 Linköping, Sweden

and L. M. W. K. Gunaratne, G. K. R. Senadeera and S. Skaarup
Physics Department, The Technical University of Denmark, DK-2800 Lyngby, Denmark

and K. West
Department of Physical Chemistry, The Technical University of Denmark, DK-2800 Lyngby, Denmark
(Received 26 June 1995)

We report studies on electronic conductivity and crystallinity in electropolymerized polypyrrole. Different growth rates during electropolymerization strongly influence and determine structural and electronic properties. Polymer films grown using low current density show higher electronic conductivity and increased crystallinity. The conductivity is also less temperature activated compared to that of the polymer grown at higher rate. X-ray diffractograms are compared to simulated diffraction data and the results are discussed in terms of increased order in the material. This may result from a different coupling route in the polymerization, induced by the lower current density. Copyright © 1996 Elsevier Science Ltd.

(Keywords: polypyrrole; conductivity; X-ray diffraction)

INTRODUCTION

Conjugated, electrically conductive, polymers have been synthesized in many different ways in recent years. The chemical constituents and the synthesizing conditions govern the final properties of the polymers. This is clearly shown for highly conducting polymers such as polyacetylene[1], where the high conductivity is intimately connected to the refined polymer synthesis. Substituted polythiophene synthesized to give high regularity shows increased conductivity[2] and crystallinity[3]. It has also been shown that polypyrrole (PPy) can attain high conductivities and even metallic properties in certain forms of the polymer[4–6]. The choice of counterion, potential control, supporting electrolyte, and polymerization temperature is crucial for the resulting material's properties[7–9].

The usual method for polypyrrole synthesis is electrochemical polymerization in which the polymerization rate can be controlled precisely. Varying the polymerization conditions by forcing geometrical constraints on the growth of polypyrrole has been shown to have a large impact on the obtained physical properties[10]. Recently we have shown that a possible explanation for this result is that the polymerization mechanisms are dependent on monomer concentration and the ratio between radicals and neutral monomers close to the surface of the growing polymer film[11]. This phenomenon, observed in a study using random arrays of recessed microelectrodes, can also be seen on macroelectrodes by controlling the polymerization rate by varying the current density. Thereby materials can be obtained with electronic properties determined by the polymerization rate, as seen from optical absorption, and electrochemical properties as shown by differences in the detailed structure of cyclic voltammograms[12,13]. The resulting polypyrrole may also have a microscopic structure determined by the current density used at the synthesis when performed in acetonitrile[14,15]. In this way we have prepared polypyrrole films showing enhanced electronic and structural properties determined by the polymerization rate.

EXPERIMENTAL

In order to produce the highly conjugated form of polypyrrole, the synthesis conditions must be carefully controlled. The polymerization was done in a solution of 0.1 M pyrrole monomer in propylene carbonate containing 0.5 M $LiClO_4$. The propylene carbonate was vacuum distilled and dried over a column of activated alumina. The pyrrole monomer was purified by distillation under nitrogen and kept cool and in the dark prior to use. Even under these conditions, the colourless compound would turn slightly yellow over a few days. The polymerization

* To whom correspondence should be addressed

was performed in an argon filled glove box, in order to exclude water rigorously. The films were formed galvanostatically on platinum or gold foil using a piece of freshly scraped lithium metal as a reference electrode, and either Pt or Ni as a counter electrode. The reference and counter electrodes were immersed in monomer-free electrolyte and separated from the working electrode by a porous membrane. The potential during synthesis was 3.7 V vs Li, corresponding to 0.8 V vs SCE. The thickness of the films (intended to be 10 μm) was regulated by the time of polymerization—from 20 min to 5 h—and was calculated assuming that 240 C cm^{-2} yields a one μm layer[16]. Two current densities were used: 125 μA cm^{-2} and 2 mA cm^{-2}. After formation, the films were rinsed thoroughly with pure propylene carbonate, in order to remove the remaining monomers. The film thicknesses were measured with a Dektak surface profilometer. With the PPy films still on the gold electrodes, X-ray diffractograms of the films were recorded using a Philips PW1710 powder diffractometer with Ni-filtered Cu Kα radiation in a $\theta - 2\theta$ configuration. The generator settings were 40 kV and 20 mA. The angle 2θ was scanned from 3 to 28°, with a step width of 0.02° and 30 s count time per step. The measurements were made in ambient atmosphere and at room temperature. PPy films not exposed to X-rays were removed from the electrodes. It was difficult to peel the polymers formed at high current densities off the metal without breaking the film. The d.c.-conductivity was measured with a four point probe in a He-cryostat at temperatures from 6 to 290 K.

RESULTS

The films synthesized at low and high current density, respectively, are clearly different as judged by the eye. The high current density film was light scattering and very brittle when handled as a free-standing film, while the low current density film had a smooth surface and could easily be peeled off the electrode in one piece. Synthesized to give the same amount of material by controlling the total charge input at the polymerization, the two films still differed in thickness. The thickness of the low current density film was 10 μm with a surface roughness of less than 100 nm. The high current density film was approx. 20 μm thick, with a variation of about $\pm$ 10 μm. These numbers correspond well with SEM pictures of the different samples. The high current density films have a distinct topography with the classical polypyrrole cauliflower appearance. The grains are approx. 10 μm in diameter. As a comparison, the low current density films appear very smooth, but with a spherulite structure extending over more than 500 μm. The different thicknesses could be explained by both different film densities and different yields in the polymerization process. Since the capacity above 3 V vs Li in cyclic voltammograms (which is a measure of the amount of reactive material) was almost the same for films made at different current densities, the most likely explanation is one involving the macroscopic structure of the film.

D.c.-conductivity

D.c.-conductivity measurements showed a higher conductivity for the slowly grown film. It had a room-temperature conductivity $\sigma_{RT} = 24\,S\,cm^{-1}$, whereas the quickly grown PPy had $\sigma_{RT} = 6\,S\,cm^{-1}$. At low temperatures there was a larger difference. For the slowly grown polymer the conductivity ratio was $\sigma(290\,K)/\sigma(6\,K) = 6.9$, whereas for the film grown at faster rate there was a stronger temperature activation of the conductivity giving $\sigma(290\,K)/\sigma(6\,K) = 24$. We did not see any sign of metallic properties above 6 K, i.e. finite or increasing conductivity as $T \rightarrow 0$, in either type of sample. This indicates that both films are in the insulating state, with respect to a possible insulator–metal transition. A plausible transport model is therefore Mott's variable range hopping (VRH), which is applicable to disordered semiconductors[17] and has also been successfully applied to conjugated polymers. *Figure 1* shows the conductivity data in the Mott VRH-form, $\ln(\sigma T^{1/2})$ as a function of $T^{-1/4}$, together with fits to the data in the temperature range 100–290 K. The fitted lines, i.e. the Mott VRH, have the form

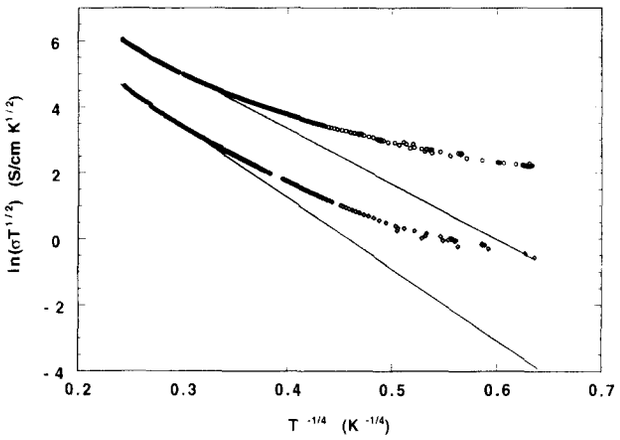

Figure 1 Mott's VRH plot of the conductivity data. The upper curve (○) is the low current density sample and the lower curve (◇) is the high current density sample. (—) Fits to the data in the temperature range 100–290 K

$$\sigma(T) = \frac{K_0}{\sqrt{T}} \exp\left(-\left(\frac{T_0}{T}\right)^{1/4}\right) \tag{1}$$

where the temperature independent parameters K_0 and T_0 are

$$K_0 = 16\,\frac{\alpha^3}{k_B N(E_F)} \tag{2}$$

$$T_0 = 0.39\sqrt{\frac{N(E_F)}{\alpha k_B}}\,\nu_0 e^2 \tag{3}$$

In these constants α^{-1} is the decay length of the wave function of the localized states, ν_0 is the hopping attempt frequency, and the other symbols have their usual meanings. Both samples deviate from the Mott VRH-model throughout the whole temperature regime. The data show a curvature where the Mott VRH predicts a straight line. The conductivity is higher than would be expected from Mott's VRH, indicating stronger contributions from other conduction processes. Using the fitted lines to extract some parameters from the data, keeping in mind their limited validity at low temperatures, we find the values of K_0 and T_0 shown in *Table 1*.

The K_0 and T_0 found are comparable to what is

Table 1 Conductivity and conductivity ratio together with parameters derived from Mott's VRH fitting to the conductivity data

Sample	$\sigma(290\,K)$ ($S\,cm^{-1}$)	$\sigma(290\,K)/\sigma(6\,K)$	K_0 ($S\,cm^{-1}K^{-1/2}$)	$T_0(K)$
$125\,\mu A\,cm^{-2}$	24	6.9	$2.8\cdot10^4$	$9.5\cdot10^4$
$2\,mA\,cm^{-2}$	6	24	$1.9\cdot10^4$	$2.2\cdot10^5$

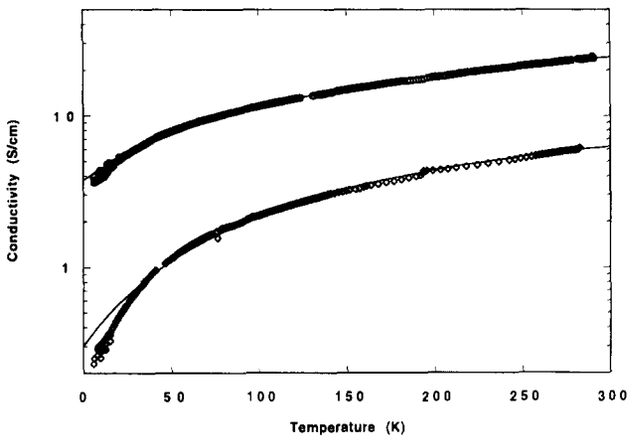

Figure 2 D.c.-Conductivity as a function of temperature in the temperature range 6–290 K. The upper curve (O) is the low current density sample and the lower curve (◇) is the high current density sample. (—) Fits to Sheng's model

observed in PPy in the insulating state[6]. We notice, however, that our samples have smaller K_0 due to the lower room temperature conductivities. From the parameters K_0 and T_0 we can find the relative decay lengths of the electronic states involved in the hopping process. If we assume a constant hopping attempt frequency and combine equations (2) and (3), we find $\alpha^{-1}_{\text{low current density}} = 1.03\,\alpha^{-1}_{\text{high current density}}$, i.e. the same decay length in both materials.

An alternative model to describe the charge transport in these materials is Sheng's fluctuation induced tunnelling conduction[18,19]. This model is based on the conduction in disordered materials containing large (> 100 nm), highly conducting regions separated by insulating barriers. The temperature dependence of the conductivity is expressed by

$$\sigma(T) = \sigma_0 \exp\left(\frac{T_1}{T_0 + T}\right) \qquad (4)$$

Table 2 Parameters derived from fitting Sheng's model to the conductivity data

Sample	$\sigma_0(S\,cm^{-1})$	$T_0(K)$	$T_1(K)$	T_1/T_0
$125\,\mu A\,cm^{-2}$	64	155	443	2.9
$2\,mA\,cm^{-2}$	19	110	456	4.2

where the parameters T_0 and T_1 are determined by the properties of the insulating barriers. In *Figure 2* the conductivity data are plotted together with fits to the Sheng model. The conductivity of the low current density sample fits well down to 20 K while the sample grown at high current density starts to deviate from this model near 40 K. The parameters from the fit are collected in Table 2. The ratio T_1/T_0 gives the slope of the curve and is determined by the barrier shape and size.

The results of the fits to the models tell us that these polypyrrole films are better described as disordered materials containing highly conducting islands, with extended electronic states, separated by insulating regions. Tunnelling between these highly conducting regions dominates the conduction process, rather than charge hopping between localized states. The higher conductivity found in the low current density sample is due to larger conducting regions and thus shorter insulating barriers to tunnel through. The apparently minor contribution from localized states is consistent with the VRH analysis giving a similar decay length of the localized states in both materials despite the different conductivities.

X-ray diffraction

X-ray diffraction measurements further support the observation of a more ordered material from the low current density synthesis. The diffractograms show that the materials are mainly amorphous. As can be seen in *Figure 3* the main reflected intensity is found between 15 and 28°, in accordance with earlier results for amorphous PPy[20]. For the slowly grown film the reflections are centred around $2\theta \approx 24°$, whereas for the film grown at the higher rate the strongest reflection occurs at $2\theta \approx 22°$.

The diffractograms show that the film grown at a high rate is totally amorphous while the slowly grown film is mainly amorphous, but with smaller distances between the polymer chains. The slowly grown film is, however,

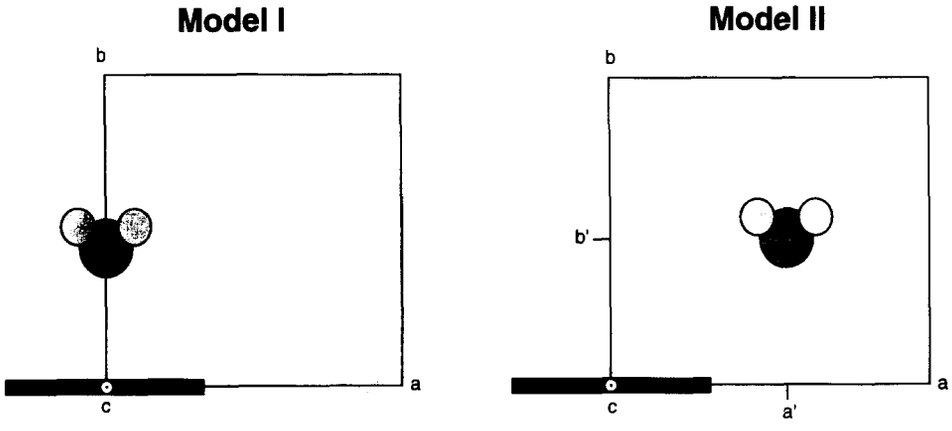

Figure 3 Schematic pictures of the two different crystal models used for X-ray diffraction simulation. The lattice cell is shown with the c-axis perpendicular to the paper and the PPy chain is depicted as a black rectangle

Table 3 Lattice patterns for the two crystal models shown in *Figure 3*

	Lattice parameters			Counter ion position			Energy
	a(Å)	b(Å)	c(Å)	a'(Å)	b'(Å)	c'(Å)	(kcal mol^{-1})
Model I	6.89	6.68	17.46	0.24	2.81	8.73	−14.5
Model II	7.37	6.78	17.46	3.91	2.76	8.95	−14.2

also partly crystalline as deduced from the sharp peaks observed at 5.3, 12.9, 17.7, and 26.3°. This corroborates the appearance of the films in SEM as previously mentioned. The background intensity below 10° makes it difficult to find peaks at small angles. Similar observations have been made in PF_6^- doped polypyrrole[21]. Our results can be compared to simulated X-ray diffractograms.

Using the molecular modelling program package Cerius[2] from Molecular Simulations Inc. we have made a geometry optimization of polypyrrole–ClO_4^- crystals, and from that we generated simulated X-ray diffractograms. We determined the geometry of the polymer chain by a Mopac calculation, using the AM1 method, and from this a unit cell was built with the polymer chain along the c-axis. The energy of the cell was then minimized by changing the lattice parameters and translating and rotating the counter ion. By comparison with the experimental diffractograms, only two crystal models were found to give diffractograms closely matching the experimental ones. Both are 20% doping level crystals (one dopant ion per five pyrrole rings), differing by the position of the counter ion. *Figure 3* shows schematic pictures of the two types and the lattice parameters are given in *Table 3*.

The simulated diffractograms are shown together with the experimental ones in *Figure 4*. As can be seen from the figure, both simulations match curve A (low current density sample), except at the 17.7° peak, which is missing in curve C (the crystal with the counter ion positioned along the b-axis). Other geometries and doping levels were investigated but none of them result in diffractograms that match the experiments.

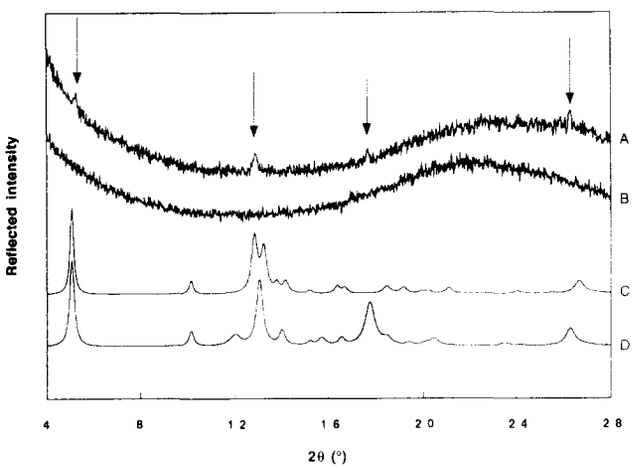

Figure 4 X-ray diffractograms from the two films and simulated diffractograms. The curves are, from the top: (A) low current density sample; (B) high current density sample; (C) simulated diffractogram from crystal model I; (D) simulated diffractogram from crystal model II

DISCUSSION

The low current density synthesis gives a more ordered material as deduced from the temperature dependence of the d.c.-conductivity and X-ray diffraction results. Sheng's conductivity model based on ordered regions separated by disordered parts is consistent with the diffraction data, which shows a greater degree of order for the sample of highest conductivity. To understand the observation of increased order from slower polymerization we turn to the analysis of the electropolymerization that we carried out in a recent work[11]. In that study we showed that geometrical constraints in the form of recessed microelectrodes influence the number of radicals available for polymerization, resulting in a lower ratio between the concentrations of radicals and neutral monomers. We then suggested that this could increase the probability of polymerization routes other than the commonly accepted radical–radical coupling[22], e.g., radical–neutral coupling[23]. As a result of this, a material with fewer defects, such as 2–3 couplings or cross-linking via the nitrogen, could be obtained. Similarly, a smaller number of radicals may be created at the polymer surface when growing at low current density. In a different polypyrrole synthesis (aqueous electrolytes), the authors suggest a chain polymerization process to explain the discrepancy between the predictions of the standard radical–radical theory and actual experimental results[24]. Comparison can also be made to the work by Schmeisser *et al.*[14], who find predominantly a 2D structure when they use a very high (3–10 mA cm^{-2}) current density in the synthesis. Their films are synthesized in acetonitrile with 0.1% of water added which could also influence the structure. The 2D films would then represent something of an opposite extreme compared to our results where we suggest one-dimensional polymer chains with fewer branching defects. A picture like this could then be suggested: low current density gives few branching defects, while the very high current density results in such a high number of branches that the material becomes a 2D network. Both extreme cases result in longer conjugation length and favourable electrical properties as compared to 'ordinary' polypyrrole. These and other examples show that the polymerization process of electropolymerized polypyrrole is still not fully understood.

CONCLUSIONS

We find a strong influence of polymerization rate on the physical properties of polypyrrole synthesized with ClO_4^- as counter-ion in propylene carbonate. The d.c.-conductivity is higher in films grown at a low current density, and fitting to the Sheng model indicates larger highly conducting, well ordered, regions compared to high current density samples. This conclusion is consistent with X-ray diffraction results that show increased crystallinity in the slowly grown film. The low current density is assumed to give a lower concentration of oxidized pyrrole monomers at the surface of the growing polypyrrole film. Thereby the coupling route for the polymerization can be given a higher probability for radical–neutral coupling than for radical–radical coupling. This could reduce the number of defects along the main chain, giving a more ordered material.

ACKNOWLEDGEMENT

This work was financially supported by the Micronics program of The Swedish Board of Technical and Industrial Developments (NUTEK).

REFERENCES

1 Naarman, H. and Theophilou, N. *Synth. Met.* 1987, **22,** 1
2 McCullough, R. D., Lowe, R. D., Jayaraman, M. and Andersson, D. L. *J. Org. Chem.* 1993, **58,** 904
3 Fell, H. J., Samuelsson, E. J., Mårdalen, J. and Andersson, M. R. *Synth. Met.* 1995, **69,** 283
4 Kohlman, R. S., Joo, J., Wang, Y. Z., Pouget, J. P., Kaneko, H., Ishiguro, T. and Epstein, A. J. *Phys. Rev. Lett.* 1995, **74,** 773
5 Yoon, C. O., Reghu, M., Moses, D. and Heeger, A. J. *Phys. Rev. B* 1994, **49,** 10851
6 Sato, K., Yamamura, M., Hagiwara, T., Murata, K. and Tokumoto, M. *Synth. Met.* 1991, **40,** 35
7 Satoh, M., Kaneto, K. and Yoshino, K. *Synth. Met.* 1986, **14,** 289
8 Kiani, M. S., Bhat, N. V., Davis, F. J. and Mitchell, G. R. *Polymer* 1992, **33,** 4113
9 Sutton, S. J. and Vaughan, A. S. *Synth. Met.* 1993, **58,** 391
10 Penner, R. M. and Martin, C. R. *J. Electrochem. Soc.* 1986, **133,** 2206
11 Granström, M., Carlberg, J. C. and Inganäs, O. *Polymer* 1995, **36,** 3191
12 West, K., Zachau-Christiansen, B., Careem, M. A. and Skaarup, S. *Synth. Met.* 1993, **55–57,** 1412
13 Skaarup, S., West, K., Zachau-Christiansen, B. and Jacobsen, T. *Synth. Met.* 1992, **51,** 267
14 Paasch, G., Schmeisser, D., Bartl, A., Naarman, H., Dunsch, L. and Göpel, W. *Synth. Met.* 1994, **66,** 135
15 Schmeisser, D., Naarman, H. and Göpel, W. *Synth. Met.* 1993, **59,** 211
16 Diaz, A. F. and Castillo, J. I. *J. Chem. Soc. Chem. Commun.* 1980, 397
17 Mott, N. F. and Davis, E. A. 'Electronic Processes in Non-crystalline Materials', Clarendon Press, Oxford, 1971
18 Sheng, P. *Phys. Rev. B* 1980, **21,** 2180
19 Sheng, P., Sichel, E. K. and Gittleman, J. L. *Phys. Rev. Lett.* 1978, **40,** 1197
20 Wernet, W., Monkenbusch, M. and Wegner, G. *Makromol. Chem. Rapid Commun.* 1984, **5,** 157
21 Nogami, Y., Pouget, J.-P. and Ishiguro, T. *Synth. Met.* 1994, **62,** 257
22 Genies, E. M., Bidan, G. and Diaz, A. F. *J. Electroanal. Chem.* 1983, **149,** 101
23 Asavapiriyanont, S., Chandler, G. K., Gunawardena, G. A. and Pletcher, D. *J. Electroanal. Chem.* 1984, **177,** 229
24 Qiu, Y.-J. and Reynolds, J. R. *J. Polym. Sci.: Part A: Polym. Chem.* 1992, **30,** 1315